Preparation of Silica/Polyurethane Nanocomposites by UV-Induced Polymerization from Surfaces of Silica

Hailin Tan, Dongzhi Yang, Ming Xiao, Jing Han, Jun Nie

State Key Laboratory of Chemical Resource Engineering, College of Materials Science and Engineering, Beijing University of Chemical Technology, Beijing 100029, People's Republic of China

ABSTRACT: UV-curable nanocomposites were prepared by the *in situ* photopolymerizaton with nanosilica obtained from sol–gel process. The photoinitiator 2-hydroxy-2-methyl-1-phenylpropane-1-one (1173) was anchored onto the surface of the nanosilica with or without methacryloxypropyltrimethoxysilane (MAPS) modification. The photopolymerization kinetics was studied by real-time Fourier transform IR (RTIR), and the microstructure and properties of the nanocomposite were investigated using transmission electron microscopy and UV–visible (UV–vis) transmistance spectra. RTIR analysis indicated that the nanocomposites without MAPS had higher curing rates and final conversion than those with MAPS. The nanocomposites with an uniformal dispersion of nanosilica had high UV–vis transmittance. © 2008 Wiley Periodicals, Inc. J Appl Polym Sci 111: 1936–1941, 2009

Key words: photopolymerization; nanocomposites; nanosilica; UV-curing

INTRODUCTION

In the past several decades, organic/inorganic nanocomposites received much attention because of the enhanced various properties including viscoelastic characteristics, fire resistance and barrier properties,[1–3] resistance to scratching, abrasion, as well as other mechanical properties. The inorganic component usually consists of nanosize mineral particles (SiO_2,[4] TiO_2, ZnO and CeO_2,[5] clay platelets[6,7]) which are randomly dispersed in a polymer matrix. Of all the ways of preparing organic/inorganic nanocomposites, the sol–gel process provides a unique opportunity under mild processing conditions such as low temperature and pressure.[8–12] The most common precursor of sol–gel reaction is the tetraethoxysilane (TEOS). However, the silica network formed by TEOS does not have a good compatibility with polymers, leading to silica domains with large particles and obvious phase separation. To prepare homogeneous hybrid materials, some coupling agents, such as methacryloxypropyltrimethoxysilane (MAPS) was chosen as one of precursors to build covalent bonds between the two phases. For example, Mammeri[13] and Hsiue[14] prepared SiO_2/polymethyl methacrylate and SiO_2/polystyrene hybrid materials, the results of which indicated that the hybrid materials with covalent chemical bonds between organic and inorganic phase have better mechanical properties than that without covalent chemical bonds.

Recently, because of eye-catching characteristic of UV-curing technology, much research focused their attention on the UV-curable nanocomposites, which combined the advantages of the UV-curing process and nanotechnology and therefore imparted some unique properties to the materials,[15,16] finally finding potential uses in fields such as coatings, printing, inks, and adhesives.[17–19] There were many reports on UV-curable nanocomposites containning clay[20–24] and nanosilica.[18,25,26] Many reports focused on the enhancement effect of the polymerizable surfactants modified clay and MAPS-modified nanosilica. Because of chemical bonds between organic and inorganic phase, materials performed good mechanical and physical properties.

The purpose of this study was monitoring the radical photopolymerization kinetics of an urethane acrylate system induced from surfaces of the silica nanoparticles obtained by *in situ* sol–gel method, investigating the effect of steric hindrance of the MAPS on photopolymerization kinetics, and the properties of the obtained photocured nanocomposites.

EXPERIMENTAL

Materials

Tetraethyl orthosilicate (TEOS) was purchased from Beijing Chemical Company of China and 3-(triethyloxysilyl) propyl methacrylate (MAPS) was donated
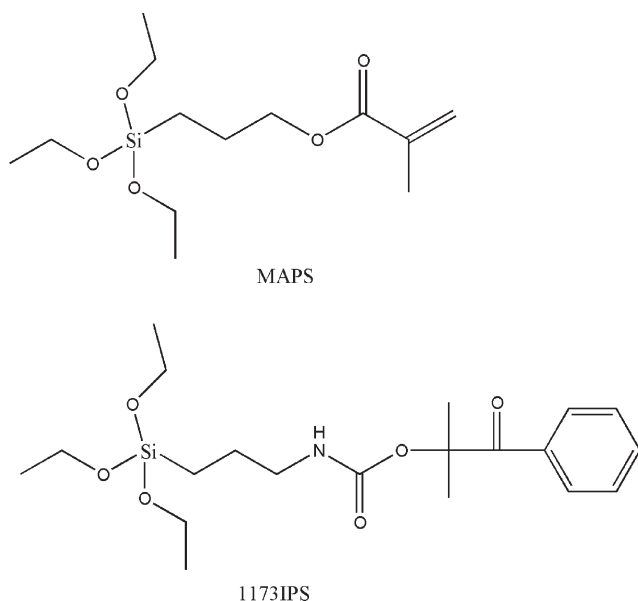
Figure 1 Structures of MAPS and 1173IPS.

by Dalian Onichem Co. Ltd. CN 962 (urethane diacrylate oligomer) and trimethylolpropane triacrylate (TMPTA) were donated by Sartomer Company. 1173IPS was synthesized by the reaction of (3-isocyanatopropyl)triethyloxysilane (IPS) and 2-hydroxy-2-methyl-1-phenylpropane-1-one (1173) in our laboratory. The structures of MAPS and 1173IPS were shown in Figure 1. All materials were used as received.

Preparation of PU/SiO$_2$ nanocomposite

The sol–gel reaction procedures for different samples were as following: CN 962 was diluted with equal volume of acetone, and the calculated TEOS, 1173IPS, MAPS and additional HCl hydrous solution were added (Si : H$_2$O : HCl (molar ratio) = 1 : 3 : 10^{-3}) and stirred for 10 min. Then, the mixture was aged for 24 h, after it was dried in vacuum. When the acetone and the water were evaporated completely, diluent TMPTA was added and stirred for 30 min. The precursors (TEOS, 1173IPS, MAPS) and the diluent were added based on weight ratio of SiO$_2$: CN962 : TMPTA (mass ratio) = 5 : 70 : 30. The 1173IPS not only played the role as silica source, but also as photoinitiator to initiate the polymerization of organic phase, and the concentrations of 1173IPS were 0.5, 1.0, 2.0, and 4.0/100 (w/w), respectively. Table I summarized the recipes for the preparation of nanocomposites and the sample codes. The symbols I and M represented the1173IPS and MAPS, respectively, and 0 and 1 indicated nanosilica without and with MAPS modification, respectively.

Characterization

Series real-time Fourier transform IR (RTIR) were recorded on a Nicolet 5700 instrument (Nicolet Instrument, Thermo Company) to determine the conversion of double bond. The mixture of composite was placed in a mold made from glass slides and spacers with 15 ± 1 mm in diameter and 1.2 ± 0.1 mm in thickness. The light intensity on the surface of samples was detected by UV Light Radiometer (Beijing Normal University, China). The double-bond conversion of the mixtures was monitored using near IR spectroscopy with the resolution of 4 cm^{-1}. The absorbance change of the =C—H peak area from 6100.70 to 6222.50 cm^{-1} was correlated to the extent of polymerization. The rate of polymerization could be calculated by the time derivative of the double-bond conversion. For each sample, the series RTIR runs were repeated three times.

Transmission electron microscopy (TEM) micrographs were taken with a Hitachi H-800 apparatus (Hitachi Corp., Tokyo). Samples were prepared by ultramicrotome at low temperature, giving nearly 100-nm thick sections.

UV–visible (UV–vis) transmittance spectra of the nanocomposites with 300–900 nm wavelengths were recorded by a UV–vis spectrophotometer (Hitachi UV-3010). The slit was set at 0.5 nm and the scan rate at 120 nm/min.

RESULTS AND DISCUSSION

Photopolymerization kinetics of nanocomposites

After sol–gel reaction procedures, the photoinitiator 1173IPS and MAPS were anchored onto the surface of the nanosilica particles. On UV exposure, the excited 1173IPS underwent homolytic cleavage resulting in the formation of free radicals, as shown schematically in Figure 2.

The free radical could initiate polymerization. Some polymerization could propagate from the nanosilica surface, and the MAPS could also

TABLE I
Recipes for Preparation of Nanocomposite

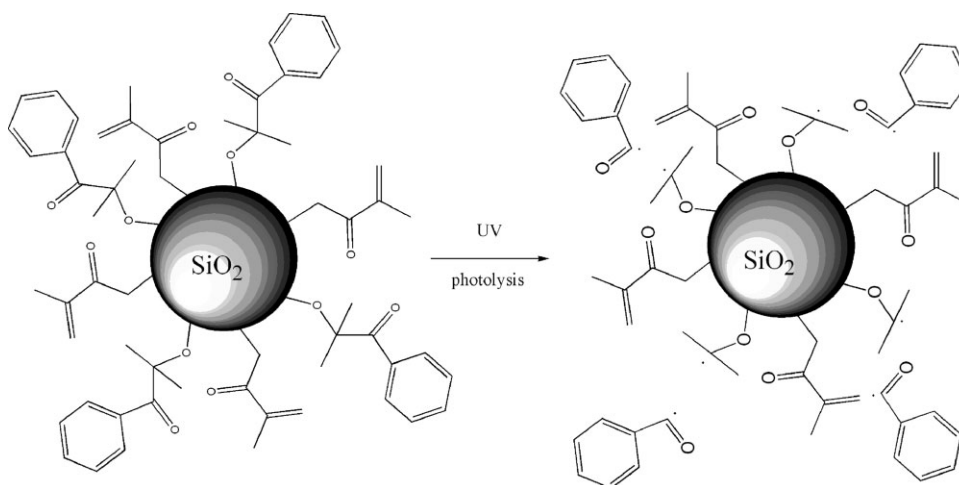| Sample code	Recipe (g)		
	1173IPS	MAPS	TEOS
I05M0	0.05	0	1.708
I05M1		0.117	1.609
I1M0	0.1	0	1.683
I1M1		0.234	1.484
I2M0	0.2	0	1.633
I2M1		0.468	1.235
I4M0	0.4	0	1.533
I4M1		0.936	0.736

The molar ratio of MAPS : 1173IPS = 4 : 1.

Figure 2   Schematic presentation of the homolytic cleavage of 1173IPS anchored onto the nanosilicas.

copolymerize with the organic matrix, which lead to the uniform dispersion of nanosilica in the polyurethane. The photopolymerization kinetics of nanocomposites was presented in Figures 3 and 4

Figure 3 showed the double-bond conversion of TEOS/1173IPS as precursor with different concentration of 1173IPS photoinitiator (0.5, 1, 2, 4/100) (w/w) as a function of irradiation time. Pure 1173, even with 0.2 wt %, had great reactivity toward the acrylate double bond, and a high degree of conversion (close to 100%) could be reached after 10 s on UV exposure. However, when the photoinitiator 1173 was anchored onto the surface of the nanosilica particles, they showed different photopolymerization kinetics. The higher the concentration of the photoinitiator, the earlier the polymerization began and the faster the rate of polymerization was, but the final double-bond conversion was very close.

When both 1173IPS and MAPS were anchored together onto the nanosilica, the homolytic cleavage radicals might initiate the polymerization of neighboring MAPS, and the photopolymerization kinetics was presented in Figure 4. With the increment of the concentration of 1173IPS, the polymerization rate increased, but the final conversion increased slightly.

To compare the photopolymerization kinetics of unmodified and modified nanosilica with MAPS, Figure 5 showed the photopolymerization kinetic curves of the nanocomposites with 2/100(w/w) and 4/100 (w/w) 1173IPS, respectively. On 20 mW/cm^2 UV exposure, the nanocomposites with and without MAPS began to polymerize after 15 s of inhibition period, and the fastest rate of polymerization was at 20 s, and after 60 s, the double-bond conversion almost came to 80%. With the increment of radiation time, the final double-bond conversion came to a
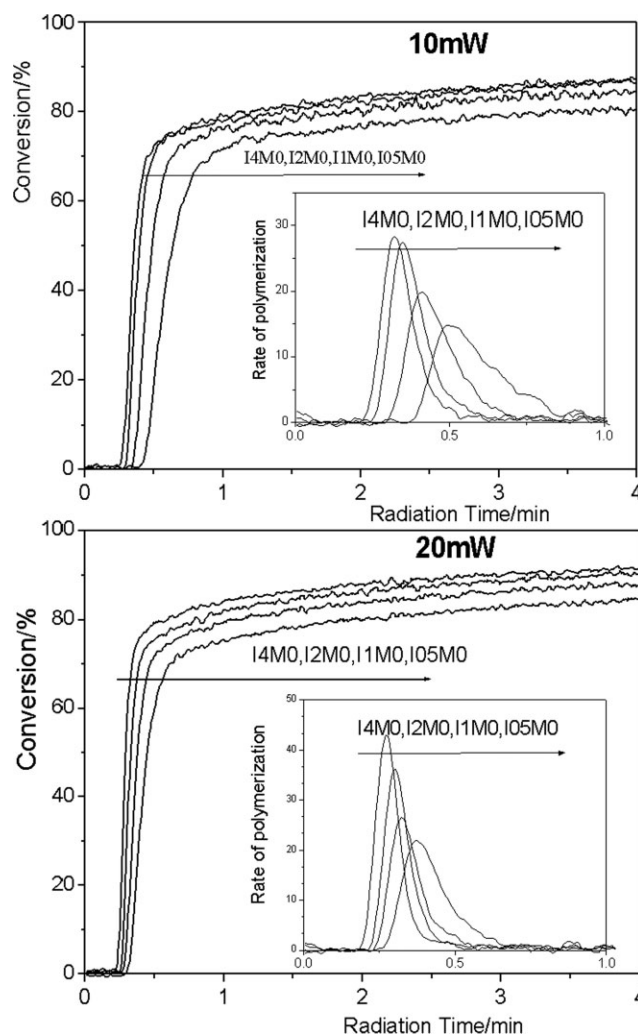

Figure 3   The double-bond conversion versus irradiation time curves of the nanocomposites without MAPS modification on 10 and 20 mW/cm^2 UV exposure.
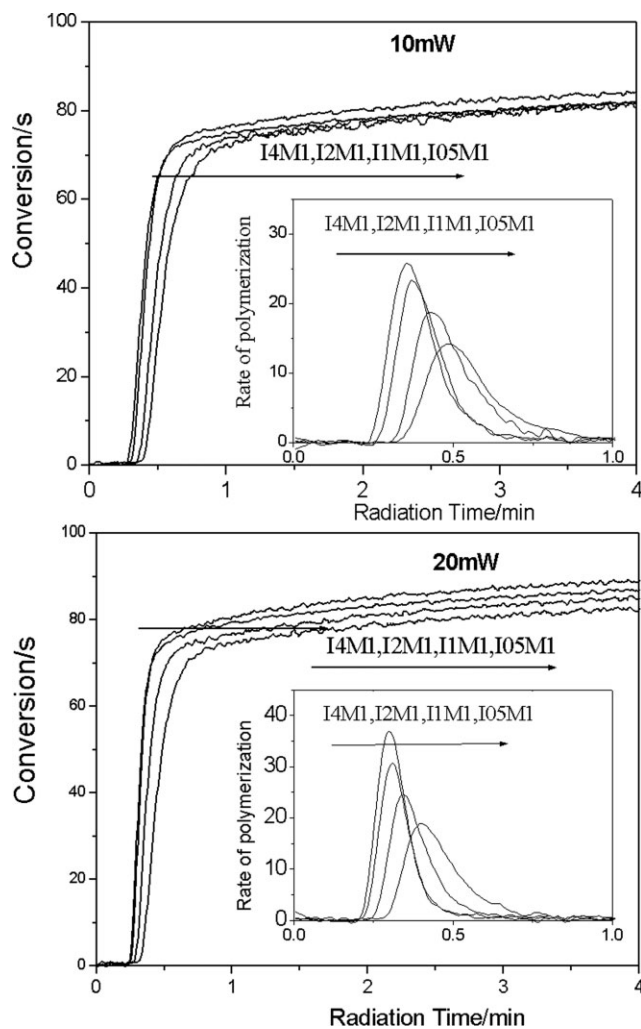
Figure 4 The double-bond conversion versus irradiation time curves of the nanocomposites with MAPS modification on 10 and 20mW/cm² UV exposure.

plateau, and the nanocomposites without MAPS had only a slightly higher final double-bond conversion than that with MAPS. The nanosilica modified with MAPS had more crosslinking sites, and during the process of polymerization, the nanocomposites with nanosilica modified by MAPS came to the gelation point earlier, which limited the movement of radicals, and leaded to the lower final double-bond conversion.

Morphology of nanocomposites

To investigate the nanocomposite structure, TEM was performed on the nanosilica/polyurethane nanocomposites. Figure 6 demonstrated the morphology of the nanocomposite prepared by the *in situ* method. The unmodified nanosilica particles could be clearly seen for TEM images. When only a little 1173IPS (0.5/100) was anchored onto the unmodified nanosilica particles, the nanosilica par-

ticles conglomerated together like cloud. With the increment of 1173IPS photoinitiator, the conglomeration was weakened and the uniformity was improved, and no phase separation took place. When the 1173IPS was 4/100 (w/w), no conglomeration could be seen, and the nanosilica uniformly dispersed in the organic matrix. When the nanosilica was modified by MAPS, the unconglomeration and uniformity were further improved. For the I4M1 samples, almost no nanosilica could be detected.

Optical properties of nanocomposites

Figure 7 showed the UV–vis transmittance spectra of the nanocomposites. The optical properties of nanocomposites are also an important parameter for their application in some fields such as optical fiber coatings, lens coatings, and so forth. In the range of 300–900 nm (visible light), about 90% transmittance for pristine polymer was observed. However, in the range of 300–400 nm (UV light), the transmittance of
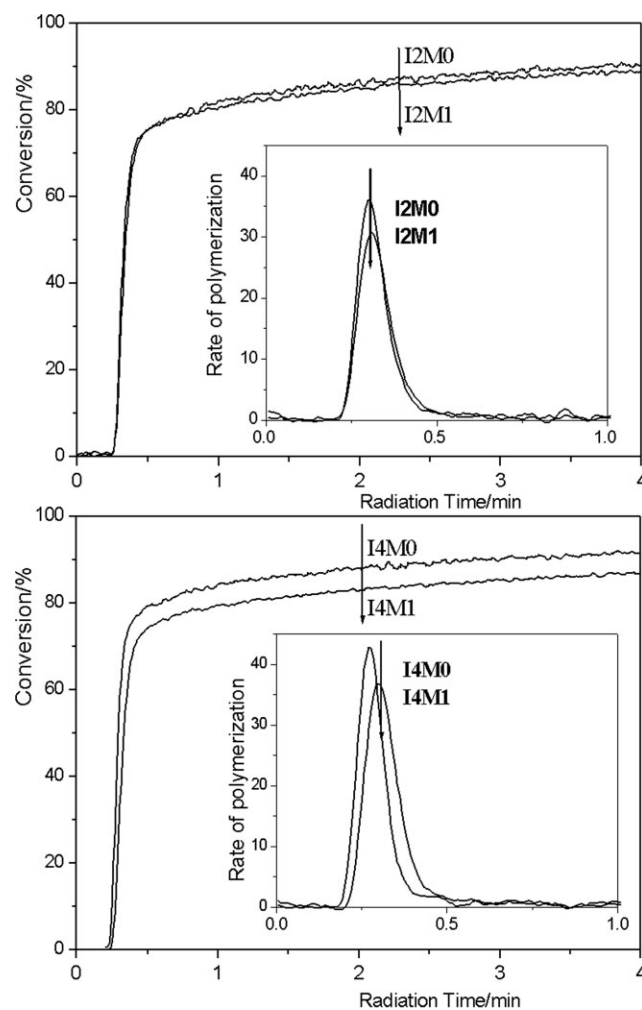

Figure 5 The double-bond conversion versus irradiation time curves of the nanocomposite with and without MAPS modification (20 mW/cm²).
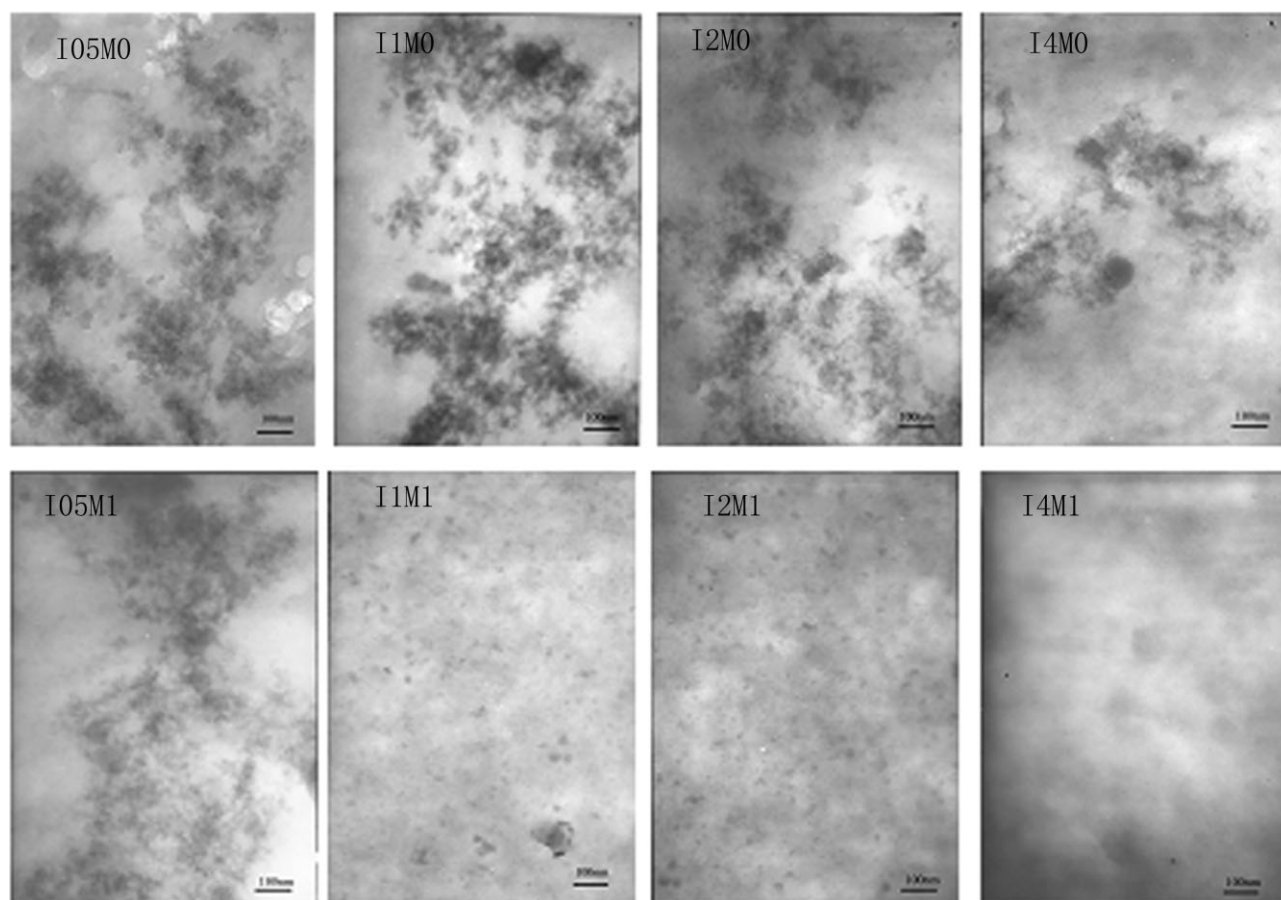
Figure 6 Morphology the of nanocomposites without and with MAPS modification.

the nanocomposites decreases dramatically. When nanosilicas were introduced into the polymer, different transmittance was observed. Combined with the morphology of nanocomposites (Fig. 6), it could be concluded that when the nanosilicas dispersed finely and uniformly in organic matrix, it had good trans-
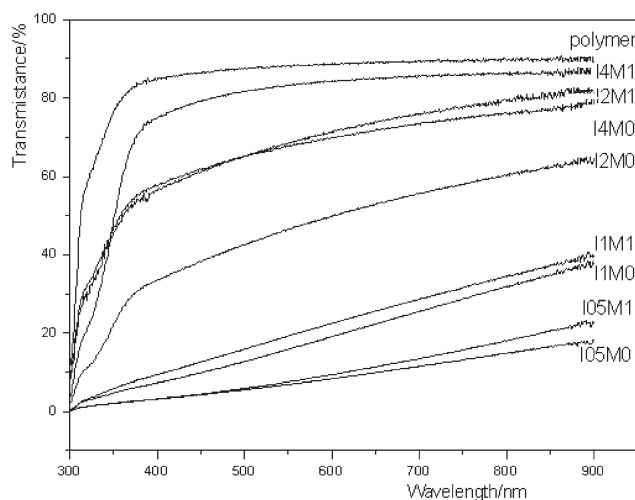
mittance. On the other hand, the modifier MAPS could improve the transmittance.

UV-curable nanocomposites were prepared by the *in situ* method. The silicate precursor of TEOS and photoinitiator 1173IPS hydrolyzed to form nanosilica particles, and the photoinitiator 1173 was anchored on the nanosilica particles with and without MAPS modification, which were evenly dispersed in the polymer matrix. The nanocomposites containing the nanosilica particles without MAPS modification had much higher curing rates than those containing the nanosilica particles with MAPS modification. MAPS and 1173IPS played an important role on the uniformal dispersion of the nanosilica in the organic matrix. It could greatly improve the UV–vis transmittance.

Figure 7 The UV–vis transmittance spectra of the nanocomposites.

References

1. Hajji, P.; David, L.; Gerard, J. F.; Pascault, J. P.; Vigier, G. J Polym Sci Part B: Polym Phys 1999, 37, 3172.
2. Liu, L. M.; Qi, Z.; Zhu, X. G. J Appl Polym Sci 1999, 71, 1133.
3. Cho, J. D.; Ju, H. T.; Hong, J. W. J Polym Sci Part A: Polym Chem 2005, 43, 658.
4. Xu, G. C.; Li, A. Y.; Zhang, L. D.; Wu, G. S.; Yuan, X. Y.; Xie, T. J Appl Polym Sci 2003, 90, 837.

5. Misra, M.; Guest, A.; Mc Tilley, M. Surf Coat Int 1998, 81, 594.
6. Carrado, K. A. Appl Clay Sci 2000, 17, 1.
7. Zhang, Q.; Fu, Q.; Jiang, L.; Lei, Y. Polym Int 2000, 48, 1561.
8. Dislich, H. Angew Chem Int Ed Engl 1971, 10, 363.
9. Mackenzie, J. D. J Non-Cryst Solids 1982, 48, 1.
10. Hench, L. L.; West, J. K. Chem Rev 1990, 90, 33.
11. Brinker, C. J.; Scherer, G. W. J Non-Cryst Solids 1985, 70, 301.
12. Mark, J. E.; Lee, C. Y.; Biancone, P. A. Hybrid Organic–Inorganic Composites (ACS Symposium Series 585); Washington, DC: American Chemical Society, 1995.
13. Mammeri, F.; Rozes, L.; Bourhis, E. L.; Sanchez, C. J Eur Ceram Soc 2006, 26, 267.
14. Hsiue, G. H.; Kuo, W. J.; Huang Y. P.; Jeng, R. J. Polymer 2000, 41, 2813.
15. Bauer, F.; Ernst, H.; Decker, U.; Findeisen, M.; Glasel, H. J.; Langguth, H.; Hartmann, E.; Mehnert, R.; Peuker, C. Macromol Chem Phys 2000, 201, 2654.
16. Muh, E.; Stieger, M.; Klee, J. E.; Frey, H.; Mulhaupt, R. J Polym Sci Part A: Polym Chem 2001, 39, 4274.
17. Wenning, A. Macromol Symp 2002, 187, 597.
18. Soppera, O.; Croutxe, B. C. J Polym Sci Part A: Polym Chem 2003, 41, 716.
19. Decker, C. Polym Int 1998, 45, 133.
20. Vollath, D.; Szabo, D. V. Adv Eng Mater 2004, 3, 117.
21. Uhl, F. M.; Davuluri, S. P.; Wong, S. C.; Webster, D. C. Chem Mater 2004, 16, 1135.
22. Decker, C.; Zahouily, K.; Keller, L.; Benfarhi, S.; Bendaikha, T.; Baron, J. J Mater Sci 2002, 37, 4831.
23. Benfarhi, S.; Decker, C.; Keller, L.; Zahouily, K. Eur Polym Mater 2004, 40, 493.
24. Hailin, T.; Jun, N.; Macromol React Eng 2007, 1, 384.
25. Sangermano, M.; Malucelli, G.; Amerio, E.; Priola, A.; Billi, E.; Rizza, G. Progr Org Coat 2005, 54, 134.
26. Fusheng, L.; Shuxue, Z.; Limin, W. J Appl Polym Sci 2005, 98, 1119.